Journal of Environmental Management 253 (2020) 109751

Contents lists available at ScienceDirect

Journal of Environmental Management

journal homepage: http://www.elsevier.com/locate/jenvman

Research article

# A WRF-Chem model-based future vehicle emission control policy simulation and assessment for the Beijing-Tianjin-Hebei region, China

Qianru Zhang [a], Peifeng Tong [a], Maodian Liu [a], Huiming Lin [a], Xiao Yun [a], Haoran Zhang [a], Wei Tao [b], Junfeng Liu [a], Shuxiao Wang [c], Shu Tao [a], Xuejun Wang [a,*]

[a] Ministry of Education Laboratory of Earth Surface Processes, College of Urban and Environmental Sciences, Peking University, Beijing, 100871, China
[b] Multiphase Chemistry Department Max-Planck-Institute for Chemistry, Hahn-Meitner-Weg 1, 55128, Mainz, Germany
[c] State Key Joint Laboratory of Environment Simulation and Pollution Control, School of Environment, Tsinghua University, Beijing, 100084, China

ARTICLE INFO

*Keywords:*
Vehicle
Emission control policies
WRF-Chem
Fine particulate matter ($PM_{2.5}$)
Surface ozone ($O_3$)

ABSTRACT

Using 2025 as the target year, we quantitatively assessed the reduction potentials of emissions of primary pollutants (including CO, HC, $NO_x$, $PM_{2.5}$ and $PM_{10}$) under different vehicle control policies and the impacts of vehicle emission control policies in the BTH region on the regional $PM_{2.5}$ concentration in winter and the surface ozone ($O_3$) concentration in summer. Comparing the different scenarios, we found that (1) vehicle control policies will bring significant reductions in the emissions of primary pollutants. Among the individual policies, upgrading new vehicle emission standards and fuel quality in Beijing, Tianjin, and Hebei will be the most effective policy, with emission reductions of primary pollutants of 26.3%–54.7%, 38.0%–70.3% and 46.0%–81.6% in 2025, respectively; (2) for $PM_{2.5}$ in winter, the Combined Scenario (CS) will lead to a reduction of 0.5–3.9 $\mu g\ m^{-3}$ (3.5%–11.6%) for the monthly average $PM_{2.5}$ concentrations in most areas. The monthly nitrate and ammonium concentrations would reduce by 5.8% and 5.3%, respectively, in the whole BTH region, indicating that vehicle emission control policies may play an important role in the reduction of $PM_{2.5}$ concentrations in winter, especially for nitrate aerosols; and (3) for $O_3$ concentrations in summer, vehicle emission control policies will lead to significant decreases. Under the CS scenario, the maximum reduction of monthly average $O_3$ concentrations in the summer is approximately 3.6 ppb (5.9%). Most areas in the BTH region have a decrease of 15 ppb (7.5%) in peak values compared to the base scenario. However, in some VOC-sensitive areas in the BTH region, such as the southern urban areas, significant reductions in $NO_x$ may lead to increases in ozone concentrations. Our results highlight that season- and location-specific vehicle emission control measures are needed to alleviate ambient $PM_{2.5}$ and $O_3$ pollution effectively in this region due to the complex meteorological conditions and atmospheric chemical reactions.

## 1. Introduction

Emissions from on-road vehicles have significant influences on the climate, air quality and public health (Greenblatt and Saxena, 2015; Tessum et al., 2014; Yan et al., 2014). It is estimated that transport sector contributed 23% of $CO_2$ emissions globally and 30% of that in Organization for Economic Cooperation and Development (OECD) countries (Ohnishi, 2008). Pollutants from vehicle exhaust emissions, such as $NO_x$ and volatile organic compounds (VOCs), are important precursors of fine particle matter ($PM_{2.5}$) and ozone throughout the troposphere, especially in urban areas (Parrish, 2006), which means that vehicular emissions are closely related to haze pollution and photochemical smoke pollution in urban areas. Vehicles also have significant effects on ambient concentrations of hazardous (Marshall et al., 2003). Therefore, vehicle emissions have been of great concern all over the world (McDonald et al., 2013; Beaton et al., 1995; Saikawa et al., 2011).

With the development of urbanization and industrialization, the number of vehicles in China has been increasing rapidly and has reached 186 million in 2016, 34-fold greater than that in 1990 (NBSC, 2017). The number is predicted to reach 400–500 million by 2030 (Wu et al., 2017). Vehicle emissions have become an important and growing source of air pollution in mega cities in China. The Beijing-Tianjin-Hebei (BTH) region is located on the North China Plain (Fig. 1). The northwestern

* Corresponding author.
*E-mail address:* xjwang@urban.pku.edu.cn (X. Wang).

https://doi.org/10.1016/j.jenvman.2019.109751
Received 26 April 2019; Received in revised form 5 September 2019; Accepted 21 October 2019
Available online 29 October 2019

area of the region is mountains, while most of the central and south-eastern areas of the region lie on the plains. The region covers 2.2% of Chinese territory, holds 8.1% of the total national population and created 10% of total national GDP in 2016. It is one of the most developed and populous regions in China. In recent years, the BTH region has suffered severe air pollution, which is mainly characterized by severe haze episodes (extremely high $PM_{2.5}$ concentrations and poor visibility) in winter (Zhang et al., 2016; Zhao et al., 2013; Zheng et al., 2015) and surface ozone pollution in summer (Lu et al., 2018; Sun et al., 2016; Wang et al., 2017). According to the China Environmental Status Bulletin (MEP, 2016a; MEP, 2017), in 2015 and 2016, the number of standard-exceeding days with $PM_{2.5}$ as the primary pollutant was the largest in the BTH region, accounting for 68.4% and 63.1% of the days, respectively, followed by ozone, accounting for 17.2% and 26.3%, respectively. Under the pressure of air quality improvement, governments in the BTH region have adopted a series of strategies and policies to control on-road vehicle emissions. For example, the Clean Air Action Plan 2013–2017 in Beijing promoted alternative fuel vehicles in the public bus fleet and the control of the number of vehicles in the city, etc.

Many studies on vehicle emission control strategies have been conducted around the world, such as in the US, Spain, France and China (Beaton et al., 1995; Lumbreras et al., 2008; Roustan et al., 2011; Saikawa et al., 2011). Roustan et al. (2011) presented a modeling study to explore the effect of the future evolution of traffic emissions on air quality in Paris, France and found that vehicle emission control technology could influence the primary and secondary particulate matter. Saikawa et al. (2011) studied the impact of China's stringent vehicle emission standards on Asian air quality and suggested that valid regulation of China's on road emission would have large benefits on the air quality of both China and East Asia. McDonald et al. (2018) indicated that in the US, the decrease of mobile source $NO_x$ emission could help meet stricter $O_3$ standards in the future. In China, many studies on vehicle emission control strategies been conducted across different spatial levels, such as national (Wu et al., 2017), regional (Liu et al., 2017a; Guo et al., 2016), and city level (Wu et al., 2011; Zhang et al., 2013, 2014, 2017a; Sun et al., 2019). For example, Wu et al. (2017) reviewed the vehicle emission controls in China, set several scenarios to estimate vehicle emission trends of major air pollutants through 2030, and provided policy suggestions for China's vehicle emission controls. Liu et al. (2017a) employed a series of scenarios to quantify the co-benefits for emissions of air pollutants and greenhouse gases under different vehicle emission controls by 2020 in the Pearl River Delta region. They found that updating emission standards was the best option for the co-benefit of air pollutants and greenhouse gas reduction in that region. Sun et al. (2019) generated various scenarios and made a comprehensive estimation of vehicle emissions in Tianjin from 2000 to 2030. Previous studies have provided useful references for the vehicle emission controls. However, most of the previous studies in China focused on the emission reduction effects of primary pollutants, the historical trends in vehicular emissions, and whether or not the policy could bring reductions in the concentrations of secondary pollutants, such as $PM_{2.5}$ in winter and $O_3$ in summer, and the size of the reductions are unclear in seriously polluted areas such as the BTH region. A series of vehicle emission control strategies have also been newly enforced in the BTH region in recent years. Thus, assessments of the effectiveness of current and possible future vehicle emission control policies on the reductions of primary pollutants and their impacts on regional air quality in the BTH region are needed.

In this study, we aimed to develop a vehicle emissions inventory for the target year of 2025 in the BTH region as a base scenario. Based on the existing policies, we designed five vehicle emission control policy scenarios for the BTH region in the target year and modeled the reductions of pollutants under different scenarios. The WRF-Chem model was applied to quantitatively evaluate the impacts of different vehicle emission control policies on air quality. This paper tends to provide policymakers with references for future vehicle emission control policy options and to understand their impacts on regional air quality in the BTH region.

## 2. Data and methods

### 2.1. Development of the base vehicle emissions inventory of 2025

The year 2025 is the last year of the 14th Five-year Plan in China and thus was selected as the target year of this study. In addition to the target year, we chose 2014 as the start year of the assessment. For the base scenario in the target year, we assumed that the population of vehicles in the BTH region would continue to increase naturally since 2014, under which the vehicle emission control policies would not be upgraded after 2014. Detailed parameters relating to the base scenario are presented in Table S3 (in the Supporting Information).

Many factors should be considered and integrated in the accurate estimation of vehicle emission (e.g., vehicle type, fuel type, meteorological factors, etc.), and a large number of data are needed (Lumbreras et al., 2014; Parrish, 2006; Wang et al., 2008). In this study, the vehicle emissions inventory in the BTH region for the target year was projected based on the bottom-up method used in our previous study of the 2014 vehicle emissions inventory in the BTH region (Yang et al., 2018). In this study, we also classified vehicles into eight types, which are light-duty passenger vehicle (LDPV), medium-duty passenger vehicle (MDPV), heavy-duty passenger vehicle (HDPV), light-duty truck (LDT), medium-duty truck (MDT), heavy-duty truck (HDT), taxi and bus.

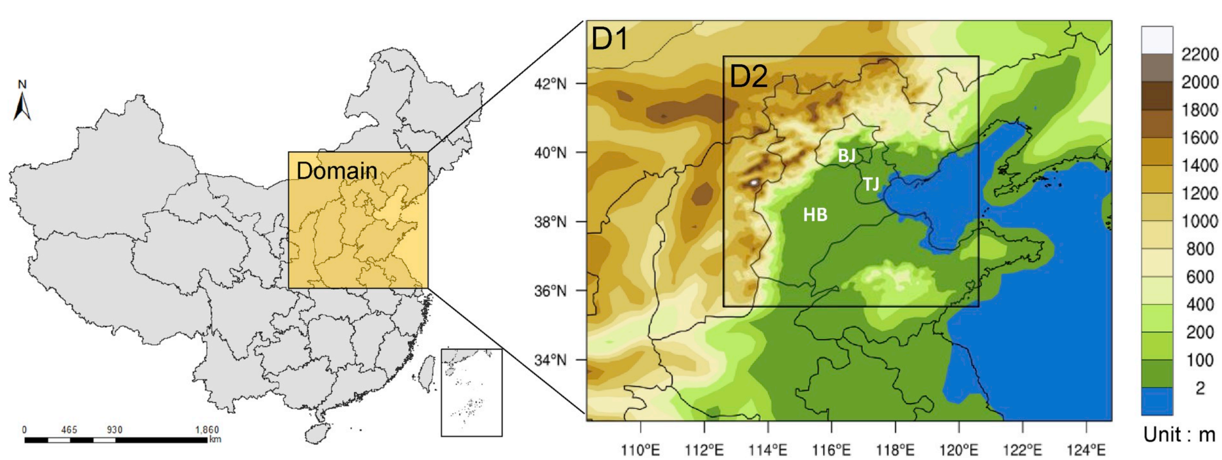


**Fig. 1.** Two domains (D1 & D2) of the WRF-Chem simulation and the terrain height of the simulation area. BJ represents Beijing, HB represents Hebei, TJ represents Tianjin.

According to the fuel type, vehicles were divided into gasoline, diesel vehicles and clean energy vehicles. Based on previous studies (Guo et al., 2016; Wang et al., 2015) and the actual commercial application of new energy vehicles in the BTH region, the clean energy vehicles included here are Hybrid Electric Vehicles (HEV), Battery Electric Vehicles (BEV), and Compressed Natural Gas Vehicles (CNGV). The vehicle emissions of CO, HC, $PM_{2.5}$, $PM_{10}$ and $NO_x$ in Beijing, Tianjin and Hebei were estimated using the following equation:

$$E_n = \sum_i \sum_j \sum_k VP_{i,j,k} \times EF_{i,j,k,n} \times VKT_{i,j} \times 10^{-6} \tag{1}$$

In equation (1), *E* represents the emissions (t) of the pollutants; *VP* is the population of vehicles; *EF* represents the emission factor (g/km); *VKT* represents the annual vehicle kilometers traveled (km), *n* represents CO, HC, $PM_{2.5}$, $PM_{10}$ and $NO_x$ in this study; *i* is the fuel types of vehicles; *j* represents the vehicle types; and *k* is the emission standard of vehicles (from China 0 to China VI).

As for the projections of vehicle population (*VP*), it is widely recognized that the population of vehicles is related to economic development. According to the elastic coefficient method (Liu et al., 2017a), we predicted the *VP* from 2015 to 2025. In this process, we used historical (2006–2014) vehicle population and economic data to reflect the relationship between the vehicle population and economy in the BTH region. The historical vehicle population and economic data were obtained from the National Bureau of Statistics of China. The GDP growth rates in the BTH region from 2015 to 2018 were obtained from the official statistics departments in Beijing, Tianjin, and Hebei. As for the prediction scenario made by Zhou et al. (2018) for GDP growth, they pointed out that in the future the GDP growth rate in the BTH region will gradually decline, so we assumed that the GDP growth rate from 2019 to 2025 would decrease to 6.5%, 6%, and 6.5% for Beijing, Tianjin, and Hebei, respectively. In this period, the GDP growth rates remain unchanged. According to the census data on vehicle population from 2015 to 2017, we compared the projected data with census data and found that the population projection method is appropriate for most vehicle types in the BTH region. For a few vehicle types with deviations greater than 10%, we added the real data from 2015 to 2017 in the elastic coefficient method to modify the projected vehicle population under the Base Scenario. The population of vehicles eliminated and newly added each year was calculated using the method of Guo et al. (2016). Here, we assumed that the newly added vehicles meet the latest emission standards in the given year (Lang et al., 2012; Sun et al., 2019).

Emission factors of different vehicles were calculated depending on the National Emission Inventory Guidebook for On-road Vehicles (Guidebook) (MEP, 2014), which was created based on lots of field measured emission factor data of vehicles in China (Wu et al., 2017). It provided a new calculation framework of vehicle emission inventory and lots of basic emission factor data. Following the Guidebook, vehicle emission factors for China 0, China I, China II, China III, China IV and China V (except China VI) in 2025 were calculated as follows:

$$EF_{i,j} = BEF_i \times \phi_j \times \gamma_j \times \lambda_i \times \theta_i \tag{2}$$

where *EF* is the emission factor (g/km), *BEF* is integrated baseline emission factor (g/km), $\phi$ represents environmental correction factor (including temperature, humidity and altitude), $\gamma$ represents average speed correction factor, $\lambda$ represents vehicle deterioration correction factor, $\theta$ represents other use condition correction factor (including load factor, fuel quality (like sulfur content) and so on), *i* represents the vehicle type, *j* represents the study area (Beijing, Tianjin, Hebei). Data used in the calculation were from the Guidebook and our previous study (Yang et al., 2018). The emission factors for China VI was modified from China V, referring to the emission limits of China V and China VI-b stages released by the Ministry of Ecology and Environment (MEP, 2016b; MEE, 2018). As for the emission factors of new energy vehicles, life cycle assessment methods have been widely applied to comprehensively evaluate the environmental impacts of electric vehicles (Tessum et al., 2014; Wang et al., 2015; Huo et al., 2013). Here, we considered the upstream well-to-tank (WTT) stage (including extraction, production, transport and delivery of fuels) and on-road tank-to-wheels (TTW) stage (e.g. vehicle operations) of HEVs and BEVs by employing localized WTT and TTW emission factors obtained from Wang et al., (2015) and Ke et al., (2017) to determine the emissions of air pollutants in power generation sector and transportation sector for HEVs and BEVs. The emission factors of CNGV were obtained from the on-road stage in the literature (Wang et al., 2015).

The *VKT* data of different vehicles was obtained from Chinese official statistics or previous literature for the BTH region. The data was listed in Table S2 (in the Supporting Information). In the function of mileage accumulation rate and vehicle age developed by Guo et al. (2007), the rate is nearly constant. Therefore, we assumed that the *VKT* of different vehicles will remain unchanged till 2025.

As for the temporal and spatial resolution of the vehicle emission inventory, we improved the temporal resolution of vehicle inventories in the BTH region for the seasonal air quality targets. Regional meteorological conditions in different months such as temperature, humidity and atmospheric pressure can significantly affect the emissions of vehicles (Weilenmann et al., 2009; Zheng et al., 2014). Based on the inventory of our previous study (Yang et al., 2018), we used the method in the National Emission Inventory Guidebook for On-road Vehicles Guidebook (MEP, 2014) to create the province-specific monthly environmental correction factors ($\phi$), in which the province-specific monthly mean temperature and humidity were calculated based on the ground meteorological observation data from China Meteorological Data Service Center. In this way, we improved the temporal resolution of vehicle inventories in the BTH region. The spatial distributions of vehicle emissions in 2025 were consistent with that of 2014, with a grid size of 1 km*1 km.

Integrating the above data and methods, we established a base vehicle emissions inventory of the target year (2025). We also used these methods to modify key parameters to get the vehicle emissions inventories of 2025 under five control scenarios defined on the next part.

### 2.2. Vehicle emission control scenarios in the BTH region

In recent years, in order to reduce the impact of vehicle emissions on air quality in the BTH region, the central and local governments have implemented a number of control strategies and policies, which include controlling LDPV population growth, upgrading emission standards for new vehicles, improving fuel quality, eliminating high-emission vehicles, introducing alternative fuels and new energy vehicles, and so on.

For instance, due to the high growth rate of LDPVs, the Beijing municipal government initiated its license control policy on the population of LDPVs in 2011 and tightened the control starting in 2014, which decreased the amount of newly added LDPVs each year from 240,000 to 150,000. Tianjin also adopted this policy in 2014 to control the amount of new LDPVs each year to less than 100,000.

China's new vehicle emission standards mainly follow European standards. Generally, in order to ensure the emissions reduction effect of vehicle emission control policies, new fuel standards and emission standards in the same region are implemented simultaneously. According to Beijing Environmental Protection Bureau (EPB), China I, China II, China III, China IV and China V were regulated for new vehicles in Beijing in 1999, 2002, 2005, 2008 and 2013, respectively. The implementation time of vehicle emission standards in Tianjin and Hebei is consistent with the national emission standards. In 2014, China IV emission standards were implemented for new light-duty gasoline vehicles and buses in Tianjin and Hebei, and China IV emission standards were also applied for new heavy-duty diesel vehicles.

Eliminating high-emission vehicles is considered to be an effective way to reduce vehicle emissions (Liu et al., 2017b). For example, the $NO_x$ emissions and PM emissions of an old pre-Euro 1 diesel bus are more than 1.5 times and 6 times that of a new Euro 3 standard diesel bus, respectively (Hao et al., 2006). For in-use high-emission vehicles, some local governments encourage car owners to scrap yellow-label vehicles (high-emission vehicles) in advance by giving financial subsidies or limiting their driving time and driving areas. Since 2003, yellow-label cars have been prohibited from entering the second ring road in Beijing, and in 2009, the prohibited driving area of yellow-label vehicles was extended to the fifth ring road.

Recently, local governments in the BTH region are encouraging the development of the clean energy vehicles, such as HEV and BEV, especially for high-use public vehicles such as taxis and buses. Governments also encourages citizens to purchase clean energy vehicles by issuing more registration licenses for clean energy vehicles and providing financial subsidies or tax reductions.

In addition, many other vehicle-related policy measures were also adopted in recent years to mitigate air pollution, which could be seen in local regulations, such as the Clean Air Action Plan 2013–2017 issued by the Beijing municipal government in September 2013.

Considering the actions taken and the policies released in the BTH region in recent years, four independent vehicle control scenarios including controlling LDPV population growth, upgrading emission standards for new vehicles and improving fuel quality, eliminating high-emission vehicles and introducing alternative fuels and new energy vehicles were established in the BTH region for the period of 2015–2025. Here, we presumed that only individual vehicle policy was updated and applied until 2025, and other policies remained unchanged in the level of 2014. In this way, we could evaluate the effects of the independent vehicle control policy in the long term. Besides the individual vehicle policies, Combined Scenario (CS) is the integration of the four independent scenarios which is expected to be implemented in the BTH region in future years. CS was established to analyze the effects of vehicle control policies in the real situation. Table 1 gives detailed descriptions of the scenarios established in this study.

### 2.3. Air quality model configuration

The migration and transformation of pollutants in the atmosphere are very complex, and air quality could be affected by meteorological factors, topographic factors, emission intensity changes, complex chemical, and photochemical reactions in the atmosphere, and so on. To assess the impacts of vehicle emission control policies on the air quality, the Weather Research and Forecasting Model coupled to chemistry (WRF-Chem) (Fast et al., 2006; Grell et al., 2005) version 3.9 was used in this study. WRF-Chem is a mesoscale online coupled meteorology-chemistry model, which considers various coupled physical and chemical processes including emission, transport, mixing, deposition, chemical transformation, aerosol interactions, photolysis, and radiation (Grell et al., 2005; Fast et al., 2006; Baklanov et al., 2014). The model combines topographic data, meteorological data, and emissions data as its input data. It is a fully coupled “online” meteorological and chemical transport model, for which the air quality components are consistent with the meteorological components in transport schemes, horizontal and vertical grids, physics schemes for subgrid-scale transport, and time steps (Grell et al., 2005). The model provides different parameterization schemes for the physical and chemical processes. As a flexible and state-of-the-art atmospheric model, it can be used for the investigation of regional air quality and interactions between atmospheric chemistry and meteorology (Yegorova et al., 2011; Zhou et al., 2019). In recent years, it was widely used in the simulation of regional air quality, including the BTH region (An et al., 2013; Bei et al., 2017; Li et al., 2018; Wang et al., 2016).

As shown in Fig. 1, in this study, two nested domains were used in the WRF-Chem simulation, which cover the North China Plain, with the BTH region in the domain’s center. The horizontal resolutions of domain1 and domain2 were 30 km and 6 km, respectively. The number of the vertical layers in the simulation was 30, and the top air pressure

**Table 1**
Designs and descriptions of the vehicle control policy scenarios in the BTH region in 2025.

| Scenario | Control Category | Region | Descriptions | References |
|---|---|---|---|---|
| Base | | Beijing<br>Tianjin<br>Hebei | Considering the natural elimination and growth of vehicles, without additional control measures until 2025, details are in Table S3 (in the Supporting Information) | |
| C1 | Controlling the growth of LDPV | Beijing | In 2014–2017, the population of new added LDPVs in Beijing is 0.15 million every year. In 2018–2025, the value is 0.1 million. | Beijing Clean Air Action Plan 2013–2017 |
| | | Tianjin | Since 2014, the population of new added LDPVs in Tianjin is 0.1 million every year. | Tianjin municipal people’s government on the implementation of the total passenger car control and management notice |
| | | Hebei | None | |
| C2 | Improving new vehicle emission standards and fuel quality | Beijing | Improving new vehicle emission standards and fuel quality gradually in the BTH region, details are in Table S4 and Table S5 (in the Supporting Information). | Beijing Environment Protection Bureau |
| | | Tianjin | | Tianjin Environment Protection Bureau |
| | | Hebei | | Hebei Provincial Environment Protection Bureau |
| C3 | Eliminating high-emission vehicles | Beijing | Yellowed labeled vehicles will be removed from the fleet by 2015. | Beijing Environment Protection Bureau |
| | | Tianjin | Yellowed labeled vehicles will be removed from the fleet by 2015. | Tianjin Environment Protection Bureau |
| | | Hebei | Yellowed labeled vehicles will be removed from the fleet by 2017. | Hebei Provincial Environment Protection Bureau |
| C4 | Encouraging the development of clean energy vehicles | Beijing | Promoting the application of clean energy vehicles in LDPVs, taxis and buses, details are in Table S6 (in the Supporting Information). | Beijing Municipal Transportation Commission; China Vehicle Environmental Management Annual Report; Beijing transportation development “13th five-year plan” |
| | | Tianjin | | Tianjin Environment Protection Bureau; Tianjin comprehensive transportation "13th five-year" management plan |
| | | Hebei | | Hebei Province new energy automobile |

(continued on next page)

Table 1 (*continued*)

| Scenario | Control Category | Region | Descriptions | References |
|---|---|---|---|---|
| | | | | industry "13th five-year" development plan (2016–2020) |
| CS | Combined scenario | Beijing Tianjin Hebei | C1+C2+C3+C4 | |

was 50 hPa. The scenario simulation for 2025 was made using the 2014 meteorological information.

In this study, the initial and boundary meteorological conditions for the simulation were generated from the National Centers for Environmental Prediction (NCEP) final gridded analysis datasets (http://rda.ucar.edu/datasets/ds083.2), and the meteorological conditions were nudged every 6 h. For the initial and boundary conditions for chemical species, we employed the 6-h output data from the Model for Ozone and Related chemical Tracers (MOZART model) to mitigate the error of the initial values. Additionally, the first 3 days of output were selected as the spin-up time and excluded from the analysis to reduce the error of the analysis. The main physical and chemical parameterizations of the WRF-Chem simulation employed in this study are listed in Table S1 (in the Supporting Information). Among these parameterizations, the aerosol module is simulated employing MADE/SORGAM scheme. Secondary organic aerosols are calculated using Secondary Organic Aerosol Model (SORGAM) (Schell et al., 2001), which could provide useful information for the evaluation of regional air quality benefits (Jiang et al., 2012; Beekmann et al., 2007).

As for the anthropogenic emissions, in addition to the vehicle inventory we developed, we used two different datasets to provide the emissions from other anthropogenic sectors, respectively. They are the PKU-FUEL inventory (http://inventory.pku.edu.cn/) for the year 2014 (Huang et al., 2014, 2015; Meng et al., 2017; Wang et al., 2014a; Zhong et al., 2017) and the Multi-resolution Emission Inventory for China (MEIC) data (http://www.meicmodel.org) for the year 2014 (Li et al., 2014). The emissions of VOCs and $NH_3$ are both provided by MEIC inventory, due to the lack of corresponding data of the PKU-FUEL inventory. Both MEIC and PKU-FUEL could be used to estimate emissions for multiple pollutants. Using multiple emission inventories in the simulation will provide more information and a useful comparison for the study. PKU-FUEL employs monthly fuel consumption data and provides the monthly emission inventories (Huang et al., 2017). Based on the monthly activity data on power generation, cement production, industrial GDP at the provincial level, monthly meteorological data such as regional monthly mean temperatures and so on, MEIC inventories generate the monthly emissions of power generation, industry, residential, transportation, and agriculture sectors (Zhang et al., 2009; Li et al., 2014, 2017; Zheng et al., 2014). Therefore, it is appropriate to use PKU-FUEL and MEIC data to provide emission values in other sectors for the seasonal air quality targets. For biogenic emissions, the data were calculated using the MEGAN model in WRF-Chem.

Besides the vehicle emission inventory, future emissions from other anthropogenic sectors for the year 2025 were projected based on the 2014 emission inventory (MEIC and PKU-FUEL inventory), which is the latest data available. Here, we employed ECLIPSE (Evaluating the Climate and Air Quality Impacts of Short-Lived Pollutants) V5a (latest version) dataset to update the emissions of other anthropogenic sectors in 2025 in the BTH region and surrounding areas. This dataset provides gridded global inventories at 0.5° spatial resolution for 11 species and 8 key sectors (http://www.iiasa.ac.at/web/home/research/researchPrograms/air/Global_emissions.html). It was developed with the GAINS (Greenhouse Gas and Air Pollution Interactions and Synergies) model, which contains substantial information about environmental policies, key sources of emissions, and further mitigation opportunities for 172 regions globally (Klimont et al., 2017). Above all scenarios in the ECLIPSE V5a dataset, the current legislation (CLE) baseline scenario considers current and planned environmental laws and extends until 2050 (Stohl et al., 2015; Klimont et al., 2019). Therefore, it was suitable to be used to reflect the emission changes over time in key sectors and the target region. Here, we calculated the emission changing rates in different species, different sectors, and different regions between the year 2015 and 2025 under the CLE baseline scenario in the ECLIPSE V5a dataset. Then we used the changing rates to modify the 2014 emission inventory accordingly and projected the emissions of other anthropogenic sectors in 2025 in the BTH region and surrounding areas.

### 2.4. Air quality model evaluation

In this study, we evaluated the model performance by using the data in 2014 to simulate the air quality and then compared the simulated results with observed data in Beijing, Tianjin and Hebei. The hourly observed data of $PM_{2.5}$ and $O_3$ concentrations were obtained from the real-time database from the China National Environmental Monitoring Center (http://106.37.208.233:20035/).

We also employed correlation coefficients (R) and normalized mean bias (NMB) (Simon et al., 2012) to evaluate the performance of the model. They are defined as follows:

$$R = \frac{\sum_{i=1}^{n}(M_i - \overline{M}) \times (O_i - \overline{O})}{\sqrt{\sum_{i=1}^{n}(M_i - \overline{M})^2}\sqrt{\sum_{i=1}^{n}(O_i - \overline{O})^2}} \tag{3}$$

$$NMB = 100\% * \frac{\sum(M_i - O_i)}{\sum O_i} \tag{4}$$

In equations (3) and (4), $\overline{M} = \frac{1}{n}\sum_{i=1}^{n} M_i$ and $\overline{O} = \frac{1}{n}\sum_{i=1}^{n} O_i$ represent the average values of individual simulated values $M_i$ and observed values $O_i$, respectively. $n$ is the number of observations.

We compared the simulated and observed data for $PM_{2.5}$ and $O_3$ in the BTH region to evaluate the performance of the WRF-Chem model. Fig. 2(a) and Fig. 2(b) show the time series comparisons of simulated and observed $PM_{2.5}$ concentrations in January 2014 and July 2014. We can see that the simulated results from WRF-Chem have similar variation trends to the observational data in the BTH region. The peaks and valleys of the observed data can be reproduced by WRF-Chem in the three regions. Nevertheless, the peaks of $PM_{2.5}$ are slightly underestimated in the simulation. Time series plots of simulated and observed surface ozone concentrations in January and July 2014 are shown in Fig. 2(c) and (d). Fig. 2(c) and (d) show that the calculated $O_3$ concentrations by WRF-Chem are in good agreement with the observed data for minimum value, maximum value and diurnal variation trends, indicating that WRF-Chem could provide relatively reasonable estimations for the emissions of ozone precursors, photochemical reactions and regional transport of surface ozone. Overall, the values of NMB and R in Fig. 2 are in the ranges of the results of previous studies (Zhang et al., 2017b, 2017c; Zhou et al., 2017). Therefore, the WRF-Chem model can reproduce the pollution characteristics of $PM_{2.5}$ and $O_3$, and it is appropriate to be used for evaluating the impacts of vehicle control policies on air quality.

## 3. Results and discussion

### 3.1. Emissions of pollutants under different scenarios in 2025

#### 3.1.1. Projection of the vehicle population and emissions of vehicles under the base scenario

In the three regions, the population of vehicles will increase continuously through 2025 (see Fig. S1 in the Supporting Information). For the growth rate of vehicles, in 2015–2025, the projected average annual growth rates of Beijing, Tianjin and Hebei are 4.0%, 5.4% and 14.5%, respectively. As a result, the population of vehicles in Beijing,

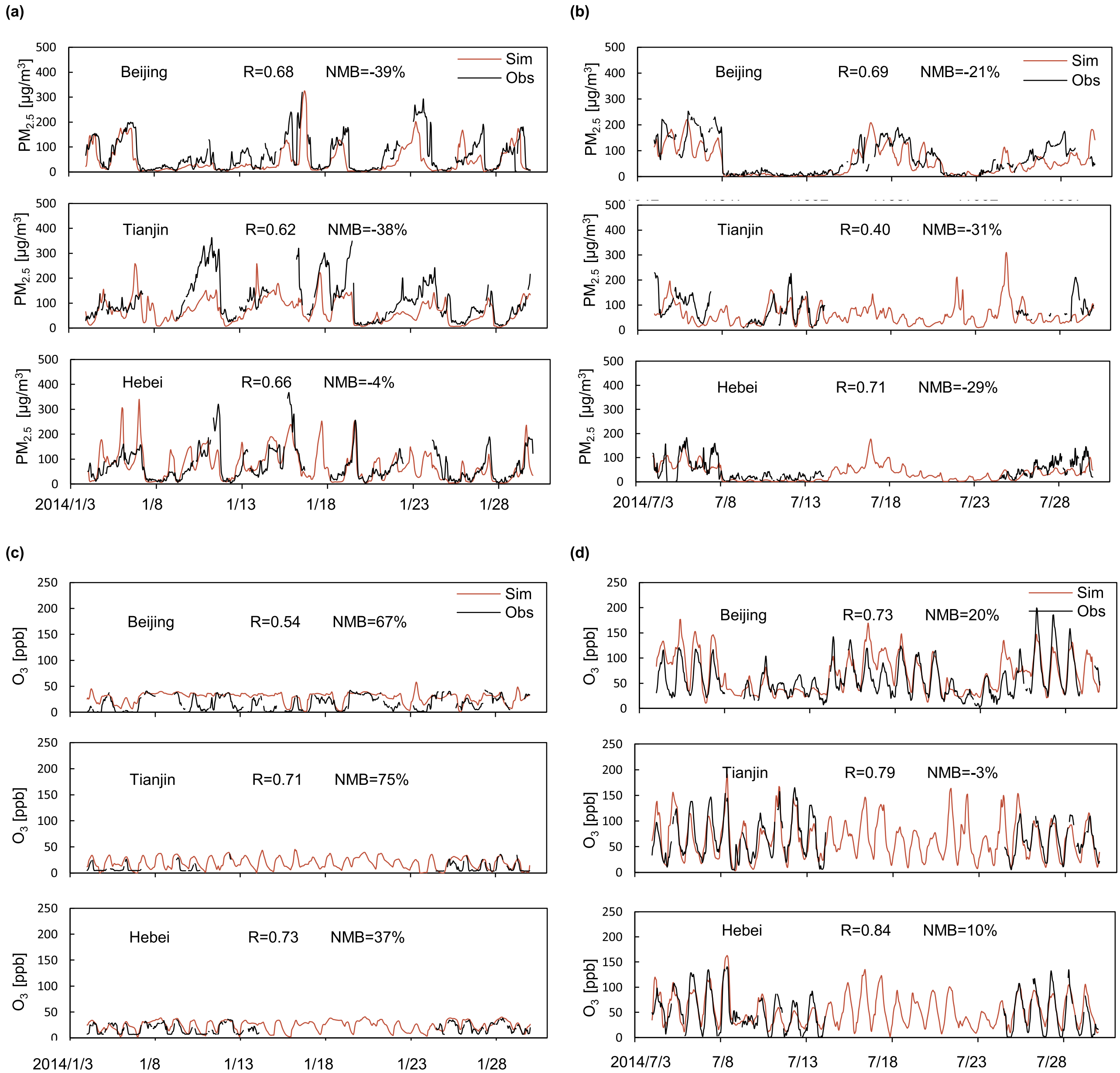


**Fig. 2.** Comparison of the simulated and observed $PM_{2.5}$ hourly concentrations in January 2014 (a) and July 2014 (b) and $O_3$ hourly concentrations in January 2014 (c) and July 2014 (d) in the BTH region.

Tianjin and Hebei in 2025 are estimated to be 8.1 million, 4.8 million and 41.1 million, respectively, under the base scenario. That means, in the future, the policymakers should pay more attention to the vehicle increase in Hebei. The rapid increase of LDPVs is the main contributor to the growth of the total population of vehicles, especially in Hebei. Due to the increase potential of private cars, the share of LDPVs in total vehicle number in Hebei will increase from 63% in 2006 to 92% in 2025. Some other vehicles will also increase slightly in the BTH region, while the population of MDTs and MDPVs will decrease slightly, which might be explained by the change of logistics mode. Hao et al. (2012) reported that the share of freight transport volume of MDTs has been and will further be taken over by HDTs and semi-trailer towing trucks due to the change of highway toll policy for trucks, the rise in oil prices and the imposition of fuel taxes.

Table 2 shows the vehicular emissions in the BTH region in 2025 under the base scenario and the emissions in 2014 under the real situation. In comparison to the vehicle emissions in 2014, the emissions of $NO_x$ in 2025 will go up. The emissions of $PM_{2.5}$ and $PM_{10}$ will decrease in Beijing because of the elimination of high-emission vehicles and the implementation of strict emission standards of China IV and China V before 2014 in Beijing. All pollutants from vehicle emissions in Hebei will increase. The increases can mainly be attributed to the increase in the population of LDPVs, HDTs and relatively slack policy on emission standards.

### 3.1.2. Comparison of emission reduction potentials under five scenarios

Table 3 shows the emission reduction potentials under five vehicle emission control scenarios compared to the base scenario in 2025. The emission contributions of difference types of vehicles under these scenarios are illustrated in Fig. 3. In Tianjin and Hebei, the most effective individual vehicle emissions control policies are adopting new vehicle standards and improving fuel quality (C2 scenario), which decrease primary pollutant emissions by 38.0%–70.3% and 46.0%–81.6%, respectively. This is caused mainly by the decreased contribution of HDTs to the emission of PM ($PM_{2.5}$ and $PM_{10}$) and LDPVs to the emission of CO.

**Table 2**
Vehicular emissions in the BTH region ($10^4$ t) in the 2025 Base Scenario and actual results from 2014.

| Region | Pollutants | Emissions ($10^4$ t) | |
|---|---|---|---|
| | | 2014 | 2025 (Base Scenario) |
| Beijing | CO | 33.19 | 36.27 |
| | HC | 3.99 | 3.66 |
| | $NO_x$ | 8.92 | 11.54 |
| | $PM_{2.5}$ | 0.32 | 0.24 |
| | $PM_{10}$ | 0.35 | 0.26 |
| Tianjin | CO | 34.42 | 30.60 |
| | HC | 3.91 | 2.82 |
| | $NO_x$ | 7.43 | 9.62 |
| | $PM_{2.5}$ | 0.38 | 0.30 |
| | $PM_{10}$ | 0.42 | 0.33 |
| Hebei | CO | 120.04 | 216.07 |
| | HC | 14.13 | 19.81 |
| | $NO_x$ | 42.21 | 72.72 |
| | $PM_{2.5}$ | 2.16 | 2.31 |
| | $PM_{10}$ | 2.40 | 2.54 |

**Table 3**
Reduction rates under the vehicle control policies in the BTH region in 2025 compared with the base scenario.

| Scenario | Region | CO | HC | $NO_x$ | $PM_{2.5}$ | $PM_{10}$ |
|---|---|---|---|---|---|---|
| C1 | Beijing | 9.9% | 10.9% | 0.9% | 4.3% | 4.0% |
| | Tianjin | 11.2% | 11.4% | 1.2% | 2.0% | 1.8% |
| | Hebei | 0.0% | 0.0% | 0.0% | 0.0% | 0.0% |
| C2 | Beijing | 26.3% | 31.0% | 50.2% | 53.9% | 54.7% |
| | Tianjin | 41.9% | 38.0% | 51.3% | 69.9% | 70.3% |
| | Hebei | 47.4% | 46.0% | 63.9% | 81.1% | 81.6% |
| C3 | Beijing | 0.7% | 0.6% | 0.1% | 0.0% | 0.0% |
| | Tianjin | 2.3% | 3.6% | 1.7% | 2.4% | 2.5% |
| | Hebei | 0.4% | 0.6% | 0.1% | 0.1% | 0.2% |
| C4 | Beijing | 12.5% | 13.8% | 7.7% | 6.8% | 6.7% |
| | Tianjin | 10.6% | 11.0% | 10.8% | 12.2% | 12.3% |
| | Hebei | 1.5% | 1.3% | 2.6% | 3.1% | 3.1% |
| CS | Beijing | 41.9% | 47.8% | 53.1% | 61.4% | 61.8% |
| | Tianjin | 52.5% | 50.8% | 56.4% | 75.0% | 75.3% |
| | Hebei | 48.5% | 47.4% | 65.9% | 82.7% | 83.3% |

Note: C1, controlling the growth of LDPV; C2, improving new vehicle emission standards and fuel quality; C3, eliminating high-emission vehicles; C4, encouraging the development of clean energy vehicles; CS, combined scenario.

For Beijing, perhaps the most effective individual policy is adopting new vehicle standards and improving fuel quality (C2 scenario), which will bring a decrease of 26.3%–54.7% for all primary pollutants in 2025, compared with the base scenario. In Beijing, developing clean energy vehicles (C4) will also bring a large decrease of all pollutants (6.7%–13.8%). Under the C4 scenario, Tianjin also has a big reduction in vehicular emissions in 2025. Under the C4 scenario, we set the proportion of clean energy vehicles based on the real situation. For LDPVs, the proportion of BEV was 75% and HEV was 25%. For taxis, the proportion of BEV was 100%. For buses, the proportion of CNGV was 50%, BEV was 45%, and HEV was 5% (Detailed information was included in Table S6 in Supporting Information). HEV has reduction effects on all pollutants and BEV could greatly reduce the emissions of $NO_X$, HC, and CO. CNGV buses could also decrease the emissions of pollutants, especially CO and $PM_{2.5}$. As shown in Fig. 3, encouraging the development of clean energy vehicles (C4) in Tianjin and Beijing will significantly reduce the contribution of taxis to the emissions of CO and HC and buses to the emissions of $NO_x$ and PM. The promotion of new energy vehicles in Hebei Province is not as strong as that in Beijing and Tianjin in the future in the C4 scenario. Therefore, the cuts in pollutants under the C4 scenario in Hebei are weak.

The license control policy (C1 scenario) for Beijing and Tianjin shows a large reduction in CO and HC, because LDPVs are the main contributor of the emissions of HC and CO in the BTH region under base scenario in 2025. Under the C1 scenario, the population of vehicles will be controlled by the number of vehicle licenses issued, compared with the base scenario.

It is reasonable that eliminating high-emission vehicles (C3 scenario) has low reductions of vehicular emissions in the BTH region in 2025. The research results of (Guo et al., 2016) showed that scrapping yellow-label vehicles might bring obvious reductions in earlier years. However, the effect would decrease gradually in the long term, because the high-emission vehicles would have been obsolete in earlier years and there are less high-emission vehicles to be scrapped.

As expected, the CS scenario leads to the biggest cuts in vehicular emissions in 2025 among all the scenarios, with a 41.9%–61.8% decrease for all the pollutants in Beijing, 50.8%–75.3% in Tianjin and 47.4%–83.3% in Hebei.

### 3.2. Air quality impacts of the vehicle emissions control scenarios in 2025

To investigate the impacts of vehicle emissions control scenarios on the air quality, we employed the WRF-Chem model to simulate $PM_{2.5}$ and $O_3$ concentrations under the base and five policy scenarios in 2025. Both MEIC and PKU-FUEL inventories were used to provide the emissions from other anthropogenic sectors, respectively. The simulation results of vehicle emission control policies using two inventories are similar with each other (see Fig. 5, Fig. 7 and Fig. S3). In this study, we mainly used the simulation results of MEIC inventory, considering the consistency of all pollutants in the study.

#### 3.2.1. $PM_{2.5}$ concentrations in winter

Fig. 4 displays the projected spatial distribution of monthly average and peak (1 h maximum) $PM_{2.5}$ concentrations in January 2025 under the base scenario. High monthly average $PM_{2.5}$ concentrations (exceeding 80 μg m$^{-3}$) could be seen in southern Hebei Province, southeast of Beijing, central Tianjin and northeast Hebei Province, where there are huge populations, heavy human activities and large anthropogenic emissions. The northwestern areas of Beijing and Hebei are mountainous areas, where the air is relative clean and the concentration of $PM_{2.5}$ is low. The research of Cai et al. (2017) has a similar simulation result for the BTH region in January 2020. The distributions of peak values of $PM_{2.5}$ concentrations in January 2025 are similar to the distributions of monthly average values. In Fig. 4, the most serious $PM_{2.5}$ pollution occurs in the southern area of Hebei, with a monthly average $PM_{2.5}$ concentration of 124 μg m$^{-3}$ and a peak value that could exceed 500 μg m$^{-3}$ in January 2025 under the base scenario.

Fig. 5(a) illustrates the projected spatial differences of monthly average $PM_{2.5}$ concentrations between the base scenario and vehicle control scenarios in the BTH region in 2025. All scenarios will bring decreases in $PM_{2.5}$ concentrations over the BTH region. As expected, the CS scenario is the most effective scenario for the reduction of $PM_{2.5}$ concentrations, with a maximum decrease of approximately 3.9 μg m$^{-3}$. Under the CS scenario, the heavily polluted areas in Fig. 4 have prominent reduction, in contrast to other areas. The reduction of monthly $PM_{2.5}$ concentration under the CS scenario of Beijing, Tianjin and Hebei is1.83, 2.62, 1.49 μg m$^{-3}$, respectively, and the reduction rate of monthly $PM_{2.5}$ concentration in the BTH region is 3.6%. We evaluated the impact of vehicle emission control policy on the components of $PM_{2.5}$ and we found that under the CS scenario, the monthly nitrate concentration and ammonium concentration would reduce 5.8% and 5.3% in the whole BTH region in January 2025, which are mainly caused by the emission reductions of $NO_x$ under the vehicle emission control policies. For individual scenarios, the C1 scenario (control policy on LDPV) leads to reductions for the entire BTH region. Relatively more reductions are seen in Beijing (0.14 μg m$^{-3}$) and Tianjin (0.21 μg m$^{-3}$) in comparison with the reduction in Hebei (0.07 μg m$^{-3}$), since the populations of LDPVs are controlled in Beijing and Tianjin under the C1 scenario. The C2 scenario (policy on introducing new vehicle emission standards and improving fuel quality) causes reductions in the northeast

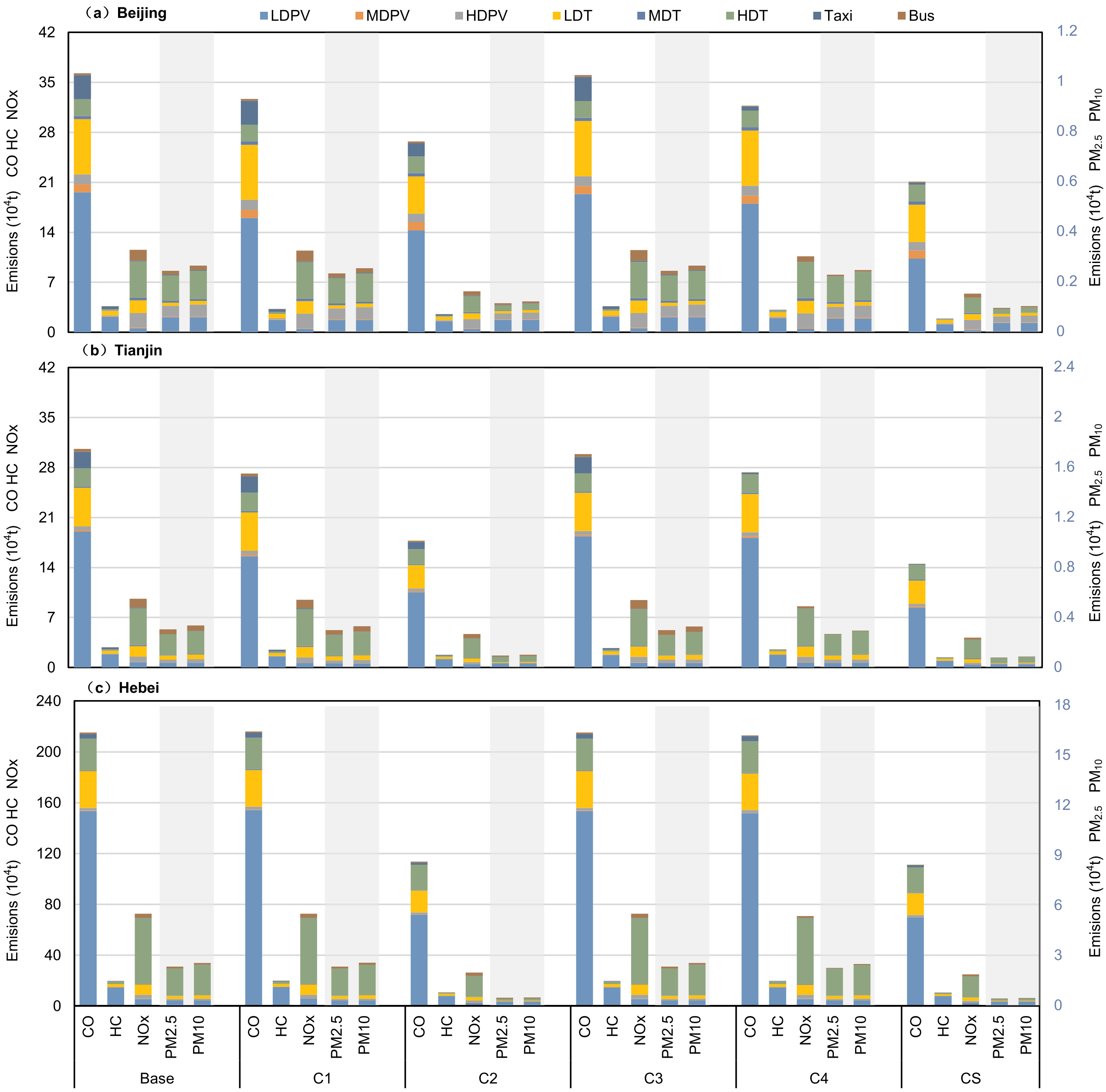


**Fig. 3.** Emission contributions of difference types of vehicles under different control scenarios in the BTH region in 2025.

area of Hebei, southeast area of Hebei, entire Tianjin and central area of Beijing, which are similar to the reductions under the CS scenario. The reduction of monthly $PM_{2.5}$ concentration under C2 scenario of Beijing, Tianjin and Hebei is 1.58, 2.27, 1.35 μg $m^{-3}$, respectively. The C3 scenario (policy on high-emission vehicle elimination) brings a very small drop of $PM_{2.5}$ concentrations in the whole BTH region, an approximate 0.03 μg $m^{-3}$ reduction of the monthly average concentration of $PM_{2.5}$. As mentioned in 3.1.2, eliminating high-emission vehicles has little effect on the reduction of emissions of pollutants in 2025, and thus, this simulation result is reasonable. The C4 scenario (policy on introducing of clean energy vehicles) leads to a limited reduction of $PM_{2.5}$ in Beijing (0.21 μg $m^{-3}$), Tianjin (0.3 μg $m^{-3}$) and Hebei (0.12 μg $m^{-3}$). A previous study (Ke et al., 2016) revealed that in the future the fleet electrification in the Yangtze River Delta region in China could have positive effects on regional air quality. Here, our results also proved that the promotion of clean energy vehicles (HEV, BEV, CNGV) could be beneficial to the improvement of regional air quality in the BTH region.

The impacts of predicted scenarios on the peak values of $PM_{2.5}$ in January 2025 are illustrated in Fig. 5(b). The distributions of the reduction of $PM_{2.5}$ peak values are different from those in Fig. 5(a). Under the CS scenario, the reduction of the $PM_{2.5}$ peak value could reach 18 μg $m^{-3}$ in many parts of the BTH region. In Fig. 5(b), the order of the effect of vehicle emission control policies on $PM_{2.5}$ peak concentrations in the BTH region from large to small is CS, C2, C4, C1and C3.

In general, $PM_{2.5}$ concentrations in winter can be influenced by the emission intensity of pollutants from local sources; a greater reduction of pollutant emissions will lead to more decrease of $PM_{2.5}$ concentration in the region. Overall, the drop of the monthly average $PM_{2.5}$ concentration is significant under the implementation of vehicle emissions control policies, indicating that vehicle emissions control policy will have a significant effect on the haze pollution reduction in winter in the future, and it will help improve air quality to a certain extent. Therefore, it's essential to implement strict control and management measures for on-road vehicles. For the peak value, in some areas, the contribution of

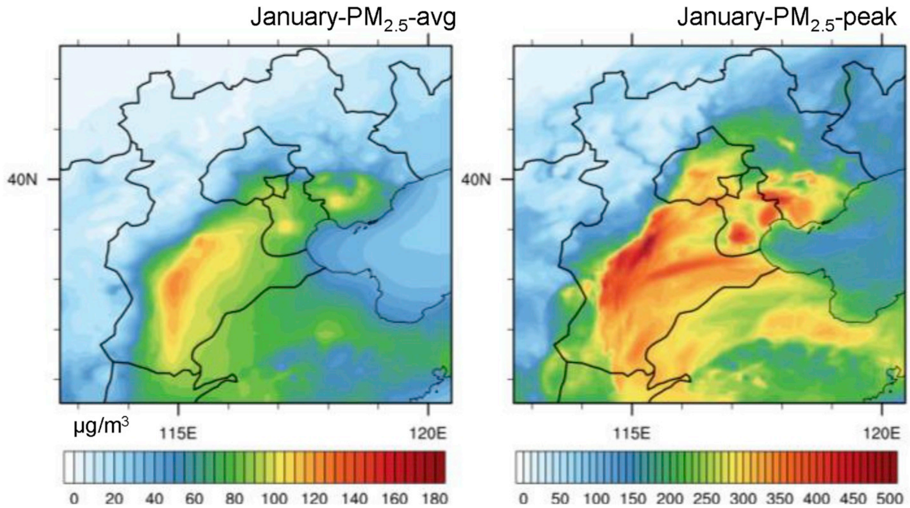


**Fig. 4.** Spatial distribution of monthly average and peak $PM_{2.5}$ concentrations in January modeled by WRF-Chem for the 2025 base scenario.

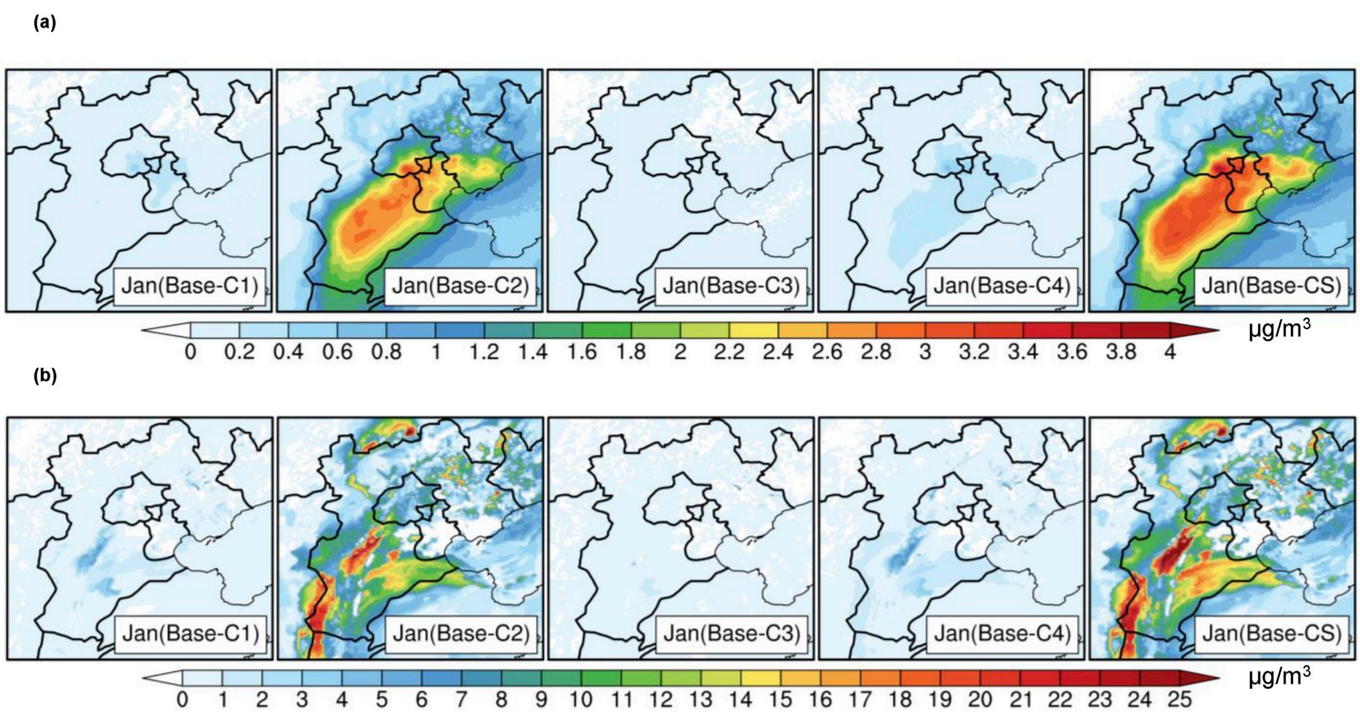


**Fig. 5.** Spatial differences of monthly average $PM_{2.5}$ concentrations (a) and peak $PM_{2.5}$ concentrations (b) between the base scenario and vehicle control scenarios in the BTH region in 2025. C1, controlling the growth of LDPV; C2, improving new vehicle emission standards and fuel quality; C3, eliminating high-emission vehicles; C4, encouraging the development of clean energy vehicles; CS, combined scenario.

vehicle emissions reductions might be relatively high, and thus, vehicle emissions control policies will play more important roles in some cases, such as in emergency pollution control in winter.

### 3.2.2. *Surface ozone concentrations in summer*

$O_3$, as a secondary pollutant, is mainly formed by the photochemical oxidation of CO and VOCs in the presence of nitrogen oxides and sunlight. For the diurnal variations of surface ozone, it usually reaches a minimum value early in the morning (2:00–6:00 local time) and reaches a maximum value at midday (approximately 15:00 local time) in the BTH region (Wang et al., 2014b). The projected spatial distributions of monthly average and maximum surface ozone concentrations in July under the base scenario in 2025 are illustrated in Fig. 6. The monthly averaged $O_3$ is higher in the northwest mountainous area and lower in the southeastern plains; this may be caused by the titration effects of high $NO_x$ emission concentrations in the urban areas (Tang et al., 2012). Almost all high peak values of $O_3$ (exceeding 180 ppb) appear in urban areas under the base scenario in July 2025. High levels of $O_3$ can be found throughout the plains, especially in Beijing and the southern area of Hebei. The maximum of peak values of hourly $O_3$ concentrations in the BTH region have exceeded 230 ppb, which is more than twice that of the second grade hourly $O_3$ concentration limit (200 μg $m^{-3}$, approximately 93 ppb) defined by China's national air quality standard.

Fig. 7(a) illustrates the spatial differences of monthly average $O_3$ concentrations between the base scenario and vehicle control scenarios in the BTH region in 2025. Under C1 scenario (control policy on LDPVs), a decrease of ozone concentration occurs throughout the whole region, the decreases in Beijing (0.21 ppb) and Tianjin (0.15 ppb) are bigger due

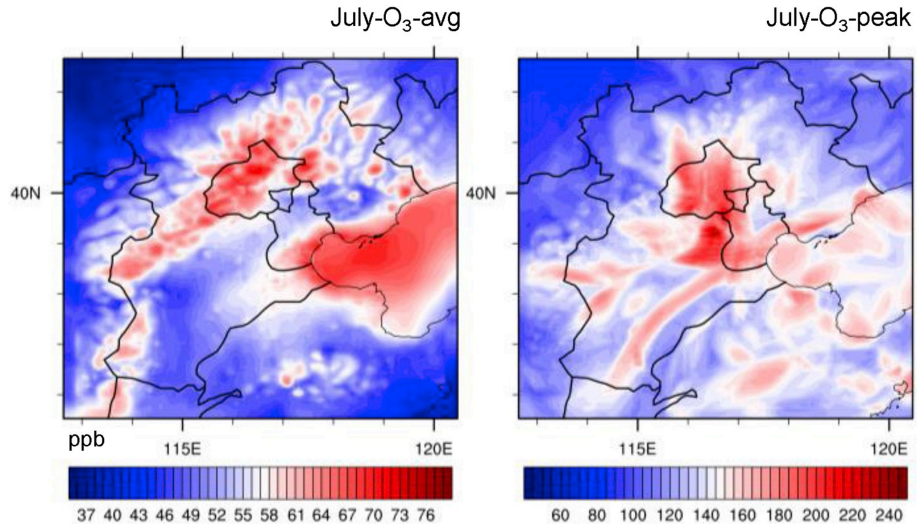


**Fig. 6.** Spatial distribution of monthly average and peak $O_3$ concentrations in July modeled by WRF-Chem for the 2025 base scenario.

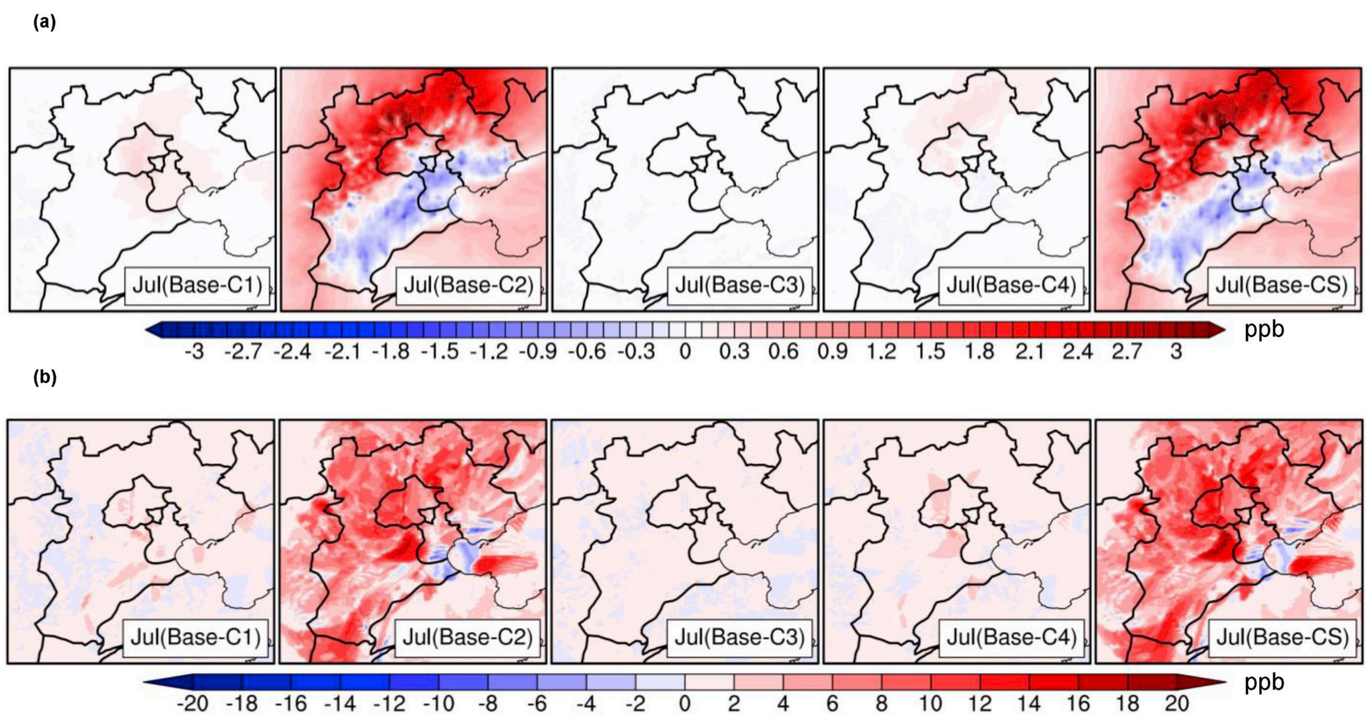


**Fig. 7.** Spatial differences of monthly average $O_3$ concentrations (a) and peak $O_3$ concentrations (b) between the base scenario and vehicle control scenarios in the BTH region in 2025. C1, controlling the growth of LDPV; C2, improving new vehicle emission standards and fuel quality; C3, eliminating high-emission vehicles; C4, encouraging the development of clean energy vehicles; CS, combined scenario.

to the implementation of license control policy on LDPVs in the two cities. Under the C2 scenario (policy on new vehicle emission standards and fuel quality) and CS, the reduction of ozone (exceed 3 ppb) is remarkable in the northwestern part of the BTH region. However, ozone concentrations in the southeastern part of the BTH region increase obviously, with a maximum increase of approximately 2 ppb. Previous studies showed that the BTH region was a VOC-sensitive region, in which the decrease of $NO_x$ and increase of VOCs could lead to the increase of ozone (Lu et al., 2018). Tang et al. (2012) also reported that ozone production in the southern plains and northern mountain areas of the BTH region was sensitive to VOCs and $NO_x$ in summer, respectively. Fig. S2 (in the Supporting Information) shows the difference in the spatial distribution of $NO_2$ concentrations between the base and five policy scenarios. We found that under the C2 and CS scenarios, the southern plains have large reductions in $NO_2$ concentrations, which is consistent with the distribution of ozone concentrations in Fig. 7(a); thus, the rising ozone concentration can be well explained in these regions. A slight decrease (less than 0.1 ppb) of ozone concentration occurs in the C3 scenario (policy on high-emission vehicles) throughout the whole region. Under scenario C4 (policy on clean energy vehicles), a decrease of $O_3$ occurs throughout Beijing (about 0.13 ppb) and Hebei Province (0.06 ppb), compared with the base scenario. However, a slight increase in $O_3$ concentrations occur in most parts of Tianjin. These regions are VOC-sensitive regions, and the phenomenon could also be explained by the strong $NO_x$ reduction.

We present the predicted spatial differences of peak values of $O_3$

concentrations between the base scenario and vehicle control scenarios in the BTH region in 2025 in Fig. 7(b). The CS scenario could provide the most significant reduction of peak ozone concentrations, with a reduction of more than 15 ppb over most parts of the BTH region. Under all the independent scenarios, the peak ozone concentrations will have evident declines in most parts of the region. The order of the effects of vehicle emission control policies on peak ozone concentrations in the BTH region from large to small is CS, C2, C4, C1, and C3.

It is clear that vehicles are the key source of $NO_x$ and an important source of VOCs; thus, vehicle emissions control policies will lead to the reduction of ozone to a certain degree. However, due to the complexity of photochemical processes in the atmosphere, the decrease of these pollutants may lead to an increase of ozone concentrations in summer.

### 3.3. Uncertainty analysis

The uncertainty of this study mainly exists in two aspects. One is the development of a vehicle emissions inventory. The other is the simulation process of WRF-Chem.

There are uncertainties in the activity data of vehicles, emission factors, and the population of vehicles. In this study, we established a vehicle emissions inventory based on mature methods, the data obtained from governmental agencies, and recent published articles. Due to the lack of adequate local data, we made some data assumptions in this study, such as simplifying the types of clean energy vehicles, which may also lead to some uncertainties in the inventory. Here, the uncertainties of HC, $NO_x$, $PM_{2.5}$, $PM_{10}$, and CO of the vehicle emissions inventory we used are −45%–67%, −52%–92%, −52%–85%, −52%–85% and −36%–49% respectively, based on the Monte Carlo method (Yang et al., 2018). We compared the vehicle emission inventories in 2014 with previous studies (Table S7 in Supporting Information), and the results suggest that the emissions in this study were in the range of results from previous studies, which proves that our method and inventories were reliable and reasonable. For the predicted vehicle emission inventories, we compared the vehicle emissions under the CS scenario in 2025 in this study with the vehicle emissions under the CLE scenario in the ECLIPSE V5a dataset in 2025 (Fig. S4 in Supporting Information) and the figure showed that our results were comparable. For other anthropogenic emission sectors, we used two different datasets to make our simulation results more reliable.

During the simulation process using the WRF-Chem model, the meteorological conditions in different years may lead to different results in emissions reductions. The sensitivity analyses for meteorological fields in 2010, 2014 and 2015 in the WRF-Chem model have proved that meteorological conditions in 2014 are suitable for the simulation of emissions reductions from control policies in China (Peng et al., 2017). In addition, the emission inventories, initial and boundary conditions, calculation methods of physical and chemical processes, as well as the accuracy of weather condition simulations could also affect the simulation results. In this study, some methods were used to attempt to reduce the uncertainties, such as setting the spin-up time and using the MOZART data to provide initial and boundary conditions for the simulation and analysis. However, due to the complex calculation processes in the chemical transport model, it's impossible to employ the traditional methods to quantify the uncertainties of simulations using the WRF-Chem model, and few studies provided definite uncertainties in their simulations.

For further studies, we expect to obtain more information about chemical reaction mechanisms to improve the analysis, and it is desirable to consider the cost and benefit in policymaking in the future.

## 4. Conclusions and recommendations

In summary, (1) among individual vehicle policies, upgrading new vehicle emission standards and fuel quality are the most effective in Beijing, Tianjin and Hebei in 2025; (2) vehicle policies will play important roles in winter for the reduction of $PM_{2.5}$ pollution, especially for the nitrate aerosols in the future; (3) for surface ozone concentrations in summer, vehicle emission control policies will lead to significant decreases. However, in some VOC-sensitive areas in the BTH region, such as the southern urban areas, significant reduction of $NO_x$ may result in the rise of ozone concentrations.

Taking $PM_{2.5}$ in winter and $O_3$ in summer as the targets of air pollution control, the implementation of stringent vehicle emissions control in both seasons is effective. In addition, due to the complex meteorological conditions and atmospheric chemical reactions, more accurate and refined strategies for different locations in the BTH region are needed.

## Acknowledgements

We greatly appreciate the reviewers' insightful comments and suggestions on the paper. This work was funded by the National Natural Science Foundation of China (No. 41571130010, 41630748, 41821005, 41571484 and 41671492) and supported by the High-performance Computing Platform of Peking University.

## Appendix A. Supplementary data

Supplementary data to this article can be found online at https://doi.org/10.1016/j.jenvman.2019.109751.

## References

An, J., Li, Y., Chen, Y., Li, J., Qu, Y., Tang, Y., 2013. Enhancements of major aerosol components due to additional HONO sources in the North China Plain and implications for visibility and haze. Adv. Atmos. Sci. 30 (1), 57–66.
Baklanov, A., Schlünzen, K., Suppan, P., Baldasano, J., Brunner, D., Aksoyoglu, S., et al., 2014. Online coupled regional meteorology chemistry models in Europe: current status and prospects. Atmos. Chem. Phys. 14 (1), 317–398.
Beaton, S.P., Bishop, G.A., Zhang, Y., Ashbaugh, L.L., Lawson, D.R., Stedmam, D.H., 1995. On-road vehicle emissions: regulations, costs, and benefits. Science 268 (5213), 991–993.
Beekmann, M., Kerschbaumer, A., Reimer, E., Stern, R., Möller, D., 2007. PM measurement campaign HOVERT in the Greater Berlin area: model evaluation with chemically specified particulate matter observations for a one year period. Atmos. Chem. Phys. 7 (1), 55–68.
Bei, N., Wu, J., Elser, M., Tian, F., Cao, J., El-Haddad, I., et al., 2017. Impacts of meteorological uncertainties on the haze formation in Beijing–Tianjin–Hebei (BTH) during wintertime: a case study. Atmos. Chem. Phys. 17 (23), 14579.
Cai, S., Wang, Y., Zhao, B., Wang, S., Chang, X., Hao, J., 2017. The impact of the "air pollution prevention and control action plan" on PM2. 5 concentrations in Jing-Jin-Ji region during 2012–2020. Sci. Total Environ. 580, 197–209.
Fast, J.D., Gustafson Jr., W.I., Easter, R.C., Zaveri, R.A., Barnard, J.C., Chapman, E.G., et al., 2006. Evolution of ozone, particulates, and aerosol direct radiative forcing in the vicinity of Houston using a fully coupled meteorology-chemistry-aerosol model. J. Geophys. Res.: Atmos 111 (D21).
Greenblatt, J.B., Saxena, S., 2015. Autonomous taxis could greatly reduce greenhouse-gas emissions of US light-duty vehicles. Nat. Clim. Chang. 5 (9), 860.
Grell, G.A., Peckham, S.E., Schmitz, R., McKeen, S.A., Frost, G., Skamarock, W.C., et al., 2005. Fully coupled "online" chemistry within the WRF model. Atmos. Environ. 39 (37), 6957–6975.
Guo, H., Zhang, Q.-y., Shi, Y., Wang, D.-h., 2007. Evaluation of the International Vehicle Emission (IVE) model with on-road remote sensing measurements. J Environ Sci 19 (7), 818–826.
Guo, X., Fu, L., Ji, M., Lang, J., Chen, D., Cheng, S., 2016. Scenario analysis to vehicular emission reduction in Beijing-Tianjin-Hebei (BTH) region, China. Environ. Pollut. 216, 470–479.
Hao, H., Wang, H., Ouyang, M., 2012. Fuel consumption and life cycle GHG emissions by China's on-road trucks: future trends through 2050 and evaluation of mitigation measures. Energy Policy 43, 244–251.
Hao, J., Hu, J., Fu, L., 2006. Controlling vehicular emissions in Beijing during the last decade. Transp. Res. A Policy Pract. 40 (8), 639–651.
Huang, T., Zhu, X., Zhong, Q., Yun, X., Meng, W., Li, B., et al., 2017. Spatial and temporal trends in global emissions of nitrogen oxides from 1960 to 2014. Environ sci amp; technol 51 (14), 7992–8000.
Huang, Y., Shen, H., Chen, H., Wang, R., Zhang, Y., Su, S., et al., 2014. Quantification of global primary emissions of $PM_{2.5}$, $PM_{10}$, and TSP from combustion and industrial process sources. Environ Sci amp; Technol 48 (23), 13834–13843.
Huang, Y., Shen, H., Chen, Y., Zhong, Q., Chen, H., Wang, R., et al., 2015. Global organic carbon emissions from primary sources from 1960 to 2009. Atmos. Environ. 122, 505–512.

Huo, H., Zhang, Q., Liu, F., He, K., 2013. Climate and environmental effects of electric vehicles versus compressed natural gas vehicles in China: a life-cycle analysis at provincial level. Environ sci amp; technol 47 (3), 1711–1718.
Jiang, F., Liu, Q., Huang, X., Wang, T., Zhuang, B., Xie, M., 2012. Regional modeling of secondary organic aerosol over China using WRF/Chem. J. Aerosol Sci. 43 (1), 57–73.
Ke, W., Zhang, S., He, X., Wu, Y., Hao, J., 2017. Well-to-wheels energy consumption and emissions of electric vehicles: mid-term implications from real-world features and air pollution control progress. Appl energy 188, 367–377.
Ke, W., Zhang, S., Wu, Y., Zhao, B., Wang, S., Hao, J., 2016. Assessing the future vehicle fleet electrification: the impacts on regional and urban air quality. Environ sci amp; technol 51 (2), 1007–1016.
Klimont, Z., Höglund-Isaksson, L., Heyes, C., Rafaj, P., Schöpp, W., Cofala, J., Purohit, P., Borken-Kleefeld, J., Kupiainen, K., Kiesewetter, G., Winiwarter, W., Amann, M., Zhao, B., Wang, S.X., Bertok, I., Sander, R., 2019. Global Scenarios of Air Pollutants and Methane: 1990-2050 (In preparation).
Klimont, Z., Kupiainen, K., Heyes, C., Purohit, P., Cofala, J., Rafaj, P., et al., 2017. Global anthropogenic emissions of particulate matter including black carbon. Atmos. Chem. Phys. 17 (14), 8681–8723.
Lang, J., Cheng, S., Wei, W., Zhou, Y., Wei, X., Chen, D., 2012. A study on the trends of vehicular emissions in the Beijing–Tianjin–Hebei (BTH) region, China. Atmos. Environ. 62, 605–614.
Li, M., Zhang, Q., Kurokawa, J.I., Woo, J.H., He, K., Lu, Z., et al., 2017. MIX: a mosaic Asian anthropogenic emission inventory under the international collaboration framework of the MICS-Asia and HTAP. Atmos. Chem. Phys. 17 (2), 935–963.
Li, M., Zhang, Q., Streets, D., He, K., Cheng, Y., Emmons, L., et al., 2014. Mapping Asian anthropogenic emissions of non-methane volatile organic compounds to multiple chemical mechanisms. Atmos. Chem. Phys. 14 (11), 5617–5638.
Li, X., Wu, J., Elser, M., Tian, F., Cao, J., El-Haddad, I., et al., 2018. Contributions of residential coal combustion to the air quality in Beijing–Tianjin–Hebei (BTH), China: a case study. Atmos. Chem. Phys. 18 (14), 10675–10691.
Liu, Y.H., Liao, W.Y., Li, L., Huang, Y.T., Xu, W.J., 2017. Vehicle emission trends in China's Guangdong Province from 1994 to 2014. Sci. Total Environ. 586, 512–521.
Liu, Y.H., Liao, W.Y., Lin, X.F., Li, L., Zeng, X.l., 2017. Assessment of Co-benefits of vehicle emission reduction measures for 2015–2020 in the Pearl River Delta region, China. Environ. Pollut. 223, 62–72.
Lu, X., Hong, J., Zhang, L., Cooper, O.R., Schultz, M., Xu, X., et al., 2018. Severe surface ozone pollution in China: a global perspective. Environ. Sci. Technol. Lett. 5 (8), 487–494.
Lumbreras, J., Borge, R., Guijarro, A., Lopez, J.M., Rodríguez, M.E., 2014. A methodology to compute emission projections from road transport (EmiTRANS). Technol. Forecast. Soc. Chang. 81, 165–176.
Lumbreras, J., Valdés, M., Borge, R., Rodríguez, M., 2008. Assessment of vehicle emissions projections in Madrid (Spain) from 2004 to 2012 considering several control strategies. Transp. Res. A Policy Pract. 42 (4), 646–658.
Marshall, J.D., Riley, W.J., McKone, T.E., Nazaroff, W.W., 2003. Intake fraction of primary pollutants: motor vehicle emissions in the South Coast Air Basin. Atmos. Environ. 37 (24), 3455–3468.
McDonald, B.C., Gentner, D.R., Goldstein, A.H., Harley, R.A., 2013. Long-term trends in motor vehicle emissions in US urban areas. Environ Sci amp; Technol 47 (17), 10022–10031.
McDonald, B., McKeen, S., Cui, Y.Y., Ahmadov, R., Kim, S.W., Frost, G.J., Graus, M., 2018. Modeling ozone in the eastern US using a fuel-based mobile source emissions inventory. Environ Sci amp; Technol 52 (13), 7360–7370.
Meng, W., Zhong, Q., Yun, X., Zhu, X., Huang, T., Shen, H., et al., 2017. Improvement of a global high-resolution ammonia emission inventory for combustion and industrial sources with new data from the residential and transportation sectors. Environ Sci amp; Technol 51 (5), 2821–2829.
Ministry of Environmental Protection, P.R.C. (MEP), 2014. National Emission Inventory Guidebook for On-Road Vehicles. MEP, Beijing (in Chinese).
Ministry of Environmental Protection, P.R.C.(MEP), 2016. China Environmental Status Bulletin. MEP, Beijing (in Chinese).
Ministry of Environmental Protection, P.R.C.(MEP), 2016. Limits and Measurement Methods for Emissions from Light-Duty Vehicles (CHINA 6). MEP, Beijing (in Chinese).
Ministry of Environmental Protection, P.R.C.(MEP), 2017. China Environmental Status Bulletin. MEP, Beijing (in Chinese).
Ministry of Ecology and Environment, P.R.C.(MEE), 2018. Limits and Measurement Methods for Emissions from Diesel Fuelled Heavy-Duty Vehicles (CHINA VI). MEP, Beijing (in Chinese).
National Bureau of Statistic of China (NBSC), 2017. China Statistical Yearbook 2017 (in Chinese).
Ohnishi, H., 2008. Greenhouse Gas Reduction Strategies in the Transport Sector: Preliminary Report. OECD/ITF, Paris.
Parrish, D.D., 2006. Critical evaluation of US on-road vehicle emission inventories. Atmos. Environ. 40 (13), 2288–2300.
Peng, W., Yang, J., Wagner, F., Mauzerall, D.L., 2017. Substantial air quality and climate co-benefits achievable now with sectoral mitigation strategies in China. Sci. Total Environ. 598, 1076–1084.
Roustan, Y., Pausader, M., Seigneur, C., 2011. Estimating the effect of on-road vehicle emission controls on future air quality in Paris, France. Atmos. Environ. 45 (37), 6828–6836.
Saikawa, E., Kurokawa, J.I., Takigawa, M., Borken-Kleefeld, J., Mauzerall, D.L., Horowitz, L.W., O'Hara, T., 2011. The impact of China's vehicle emissions on regional air quality in 2000 and 2020: a scenario analysis. Atmos. Chem. Phys. 11, 9465–9484.
Schell, B., Ackermann, I.J., Hass, H., Binkowski, F.S., Ebel, A., 2001. Modeling the formation of secondary organic aerosol within a comprehensive air quality model system. J. Geophys. Res.: Atmos 106 (D22), 28275–28293.
Simon, H., Baker, K.R., Phillips, S., 2012. Compilation and interpretation of photochemical model performance statistics published between 2006 and 2012. Atmos. Environ. 61, 124–139.
Stohl, A., Aamaas, B., Amann, M., Baker, L.H., Bellouin, N., Berntsen, T.K., et al., 2015. Evaluating the climate and air quality impacts of short-lived pollutants. Atmos. Chem. Phys. 15 (18), 10529–10566.
Sun, L., Xue, L., Wang, T., Gao, J., Ding, A., Cooper, O.R., et al., 2016. Significant increase of summertime ozone at mount tai in central eastern China. Atmos. Chem. Phys. 16 (16), 10637–10650.
Sun, S., Zhao, G., Wang, T., Jin, J., Wang, P., Lin, Y., et al., 2019. Past and future trends of vehicle emissions in Tianjin, China, from 2000 to 2030. Atmos. Environ. 209, 182–191.
Tang, G., Wang, Y., Li, X., Ji, D., Hsu, S., Gao, X., 2012. Spatial-temporal variations in surface ozone in Northern China as observed during 2009–2010 and possible implications for future air quality control strategies. Atmos. Chem. Phys. 12 (5), 2757–2776.
Tessum, C.W., Hill, J.D., Marshall, J.D., 2014. Life cycle air quality impacts of conventional and alternative light-duty transportation in the United States. Proc. Natl. Acad. Sci. 111 (52), 18490–18495.
Wang, H., Chen, C., Huang, C., Fu, L., 2008. On-road vehicle emission inventory and its uncertainty analysis for Shanghai, China. Sci. Total Environ. 398 (1–3), 60–67.
Wang, L., Zhang, Y., Wang, K., Zheng, B., Zhang, Q., Wei, W., 2016. Application of weather research and forecasting model with chemistry (WRF/chem) over northern China: sensitivity study, comparative evaluation, and policy implications. Atmos. Environ. 124, 337–350.
Wang, R., Tao, S., Balkanski, Y., Ciais, P., Boucher, O., Liu, J., et al., 2014. Exposure to ambient black carbon derived from a unique inventory and high-resolution model. Proc. Natl. Acad. Sci. 111 (7), 2459–2463.
Wang, R., Wu, Y., Ke, W., Zhang, S., Zhou, B., Hao, J., 2015. Can propulsion and fuel diversity for the bus fleet achieve the win–win strategy of energy conservation and environmental protection? Appl. Energy 147, 92–103.
Wang, T., Xue, L., Brimblecombe, P., Lam, Y.F., Li, L., Zhang, L., 2017. Ozone pollution in China: a review of concentrations, meteorological influences, chemical precursors, and effects. Sci. Total Environ. 575, 1582–1596.
Wang, Y., Hu, B., Ji, D., Liu, Z., Tang, G., Xin, J., et al., 2014. Ozone weekend effects in the Beijing–Tianjin–Hebei metropolitan area, China. Atmos. Chem. Phys. 14 (5), 2419–2429.
Weilenmann, M., Favez, J.Y., Alvarez, R., 2009. Cold-start emissions of modern passenger cars at different low ambient temperatures and their evolution over vehicle legislation categories. Atmos. Environ. 43 (15), 2419–2429.
Wu, Y., Wang, R., Zhou, Y., Lin, B., Fu, L., He, K., Hao, J., 2011. On-road vehicle emission control in Beijing: past, present, and future. Environ Sci amp; Technol 45 (1), 147–153.
Wu, Y., Zhang, S., Hao, J., Liu, H., Wu, X., Hu, J., et al., 2017. On-road vehicle emissions and their control in China: a review and outlook. Sci. Total Environ. 574, 332–349.
Yan, F., Winijkul, E., Streets, D.G., Lu, Z., Bond, T.C., Zhang, Y., 2014. Global emission projections for the transportation sector using dynamic technology modeling. Atmos. Chem. Phys. 14 (11), 5709–5733.
Yang, W., Yu, C., Yuan, W., Wu, X., Zhang, W., Wang, X., 2018. High-resolution vehicle emission inventory and emission control policy scenario analysis, a case in the Beijing-Tianjin-Hebei (BTH) region, China. J. Clean. Prod. 203, 530–539.
Yegorova, E.A., Allen, D.J., Loughner, C.P., Pickering, K.E., Dickerson, R.R., 2011. Characterization of an eastern US severe air pollution episode using WRF/Chem. J. Geophys. Res.: *Atmos* 116 (D17).
Zhang, Q., Streets, D.G., Carmichael, G.R., He, K.B., Huo, H., Kannari, A., et al., 2009. Asian emissions in 2006 for the NASA INTEX-B mission. Atmos. Chem. Phys. 9 (14), 5131–5153.
Zhang, S., Wu, Y., Liu, H., Wu, X., Zhou, Y., Yao, Z., et al., 2013. Historical evaluation of vehicle emission control in Guangzhou based on a multi-year emission inventory. Atmos. Environ. 76, 32–42.
Zhang, S., Wu, Y., Wu, X., Li, M., Ge, Y., Liang, B., et al., 2014. Historic and future trends of vehicle emissions in Beijing, 1998–2020: a policy assessment for the most stringent vehicle emission control program in China. Atmos. Environ. 89, 216–229.
Zhang, S., Wu, Y., Zhao, B., Wu, X., Shu, J., Hao, J., 2017. City-specific vehicle emission control strategies to achieve stringent emission reduction targets in China's Yangtze River Delta region. J Environ Sci 51, 75–87.
Zhang, Y., Zhu, B., Gao, J., Kang, H., Yang, P., Wang, L., et al., 2017. The source apportionment of primary $PM_{2.5}$ in an aerosol pollution event over Beijing-Tianjin-Hebei region using WRF-Chem, China. Aerosol Air Qual Res 17, 2966–2980.
Zhang, Z., Wang, W., Cheng, M., Liu, S., Xu, J., He, Y., et al., 2017. The contribution of residential coal combustion to PM2. 5 pollution over China's Beijing-Tianjin-Hebei region in winter. Atmos. Environ. 159, 147–161.
Zhang, Z., Zhang, X., Gong, D., Kim, S.-J., Mao, R., Zhao, X., 2016. Possible influence of atmospheric circulations on winter haze pollution in the Beijing–Tianjin–Hebei region, northern China. Atmos. Chem. Phys. 16 (2), 561–571.
Zhao, X., Zhao, P., Xu, J., Meng, W., Pu, W., Dong, F., et al., 2013. Analysis of a winter regional haze event and its formation mechanism in the North China Plain. Atmos. Chem. Phys. 13 (11), 5685–5696.
Zheng, B., Huo, H., Zhang, Q., Yao, Z.L., Wang, X.T., Yang, X.F., et al., 2014. High-resolution mapping of vehicle emissions in China in 2008. Atmos. Chem. Phys. 14 (18), 9787–9805.

Zheng, G., Duan, F., Su, H., Ma, Y., Cheng, Y., Zheng, B., et al., 2015. Exploring the severe winter haze in Beijing: the impact of synoptic weather, regional transport and heterogeneous reactions. Atmos. Chem. Phys. 15 (6), 2969–2983.
Zhong, Q., Huang, Y., Shen, H., Chen, Y., Chen, H., Huang, T., et al., 2017. Global estimates of carbon monoxide emissions from 1960 to 2013. Environ. Sci. Pollut. Control Ser. 24 (1), 864–873.
Zhou, G., Xu, J., Xie, Y., Chang, L., Gao, W., Gu, Y., et al., 2017. Numerical air quality forecasting over eastern China: an operational application of WRF-Chem. Atmos. Environ. 153, 94–108.
Zhou, J., Jin, B., Du, S., Zhang, P., 2018. Scenario analysis of carbon emissions of Beijing-tianjin-hebei. Energies 11 (6), 1489.
Zhou, M., Zhang, L., Chen, D., Gu, Y., Fu, T.M., Gao, M., et al., 2019. The impact of aerosol-radiation interactions on the effectiveness of emission control measures. Environ. Res. Lett. 14, 024002.